Inorg. Chem. **2007**, *46*, 9700–9707

Ligand-Induced Interconversion of a Coordination-Organized Porphyrin Dimer: a Potential Fluorescence-Based Molecular Memory Monitor

Akiharu Satake,* Junichi Tanihara, and Yoshiaki Kobuke*

Graduate School of Materials Science, Nara Institute of Science and Technology, Takayama 8916-5, Ikoma, Nara 630-0192, Japan

Received May 24, 2007

A novel interconversion system between less-fluorescent *stacked* (S) dimer and fluorescent *extended* (E) dimer of the monoimidazolylbisporphyrinatozinc complex was investigated. The addition of pyridine induces transformation from the S to the E dimer, whereas the addition of acetic acid and subsequent heating reverses the transformation. The interconversion rate is controlled by ligand concentration and thermal treatment. The system can be applied to repeatedly readable molecular memory by highly sensitive fluorescence detection.

Introduction

Switch and memory functions based on structural changes of molecules and supramolecules are of great interest as devices that operate on the molecular scale.[1] A large change in spectroscopic features is desirable for the most sensitive detection. Because of its high sensitivity, fluorescence is a clever choice of detection when a limited number of molecules are concerned, as in cases of molecular memory.[2] Combinations of chromophores with appropriate energy acceptors or electron donors (or acceptors) are frequently used to detect outer stimuli via flouresence resonance energy transfer (FRET) or photoinduced electron transfer processes. The change of the conjugation state of π-conjugated molecules by outer ligands[3] and light[4] causes a change in both absorption and fluorescence spectra. Although the latter photochromism is effective for rapid information writing, its isomerizing nature on photoirradiation leaves a problem for readout by fluorescence. Nondestructive fluorescence detection of photochromic systems have been investigated continuously by combination with FRET[5] or excited-state intermolecular proton transfer.[6]

Aggregation and change of the aggregation states of luminescent materials are another strategy for fluorescence-based molecular devices.[7] It is well-known that *H*-type aggregates are less fluorescent than *J*-type aggregates due to nonradiative pathways formed by face-to-face interactions.[8] In addition, the UV−vis spectra of *H*- and *J*-type aggregates are different due to excitonic coupling caused by different chromophoric arrangements.[9] If the aggregation states are controlled by outer stimuli, the system can be applied to molecular memory applications that show differences in absorption and emission spectra.[7a,10] Change of aggregation states by thermal operation has previously been reported for fluorescent dyes in lipid membrane[11] and self-assembled phosphorescent metal complexes.[12] In these cases, however, significant numbers of molecules are involved with

* To whom correspondence should be addressed. E-mail: satake@ms.nasit.jp (A.S.), kobuke@iae.kyoto-u.ac.jp (Y.K.). Phone: +81-743-726113 (A.S.). Fax: +81-743-72-6119 (A.S.).

(1) (a) Balzani, V.; Scandola, F. *Supramolecular Photochemistry*; Ellis Horwood: New York, 1991. (b) Lehn, J.-M. *Supramolecular Chemistry: Concepts and Perspectives*; VCH: Weinheim, Germany, 1995. (c) Ben Feringa, L. *Molecular Switches*; Wiley: Weinheim, Germany, 2001.

(2) Valeur, B. *Molecular Fluorescence*; Wiley-VCH: Weinheim, Germany, 2002.

(3) (a) McQuade, D. T.; Pullen, A. E.; Swager, T. M. *Chem. Rev.* **2000**, *100*, 2537. (b) Wang, B.; Wasielewski, M. R. *J. Am. Chem. Soc.* **1997**, *119*, 12. (c) Shinmori, H.; Ahn, T. K.; Cho, H. S.; Kim, D.; Yoshida, N.; Osuka, A. *Angew. Chem., Int. Ed.* **2003**, *42*, 2754. (d) Kitagishi, H.; Satake, A.; Kobuke, Y. *Inorg. Chem.* **2004**, *43*, 3394.

(4) (a) Brown, G. H. *Photochromism*; Wiley-Interscience: New York, 1971. (b) Irie, M. *Chem. Rev.* **2000**, *100*, 1685. (c) Dürr, H.; Bouas-Laurent, H. *Photochromism: Molecules, Systems*; Elsevier: Amsterdam, 2003. (d) Matsuda, K.; Irie, M. *J. Photochem. Photobiol., C* **2004**, *5*, 169. (e) Gust, D.; Moore, T. A.; Moore, A. L. *Chem. Commun.* **2006**, 1169.

(5) (a) Giordano, L.; Jovin, T. M.; Irie, M.; Jares-Erijman, E. A. *J. Am. Chem. Soc.* **2002**, *124*, 7481. (b) Guo, X.; Zhang, D.; Zhou, Y.; Zhu, D. *J. Org. Chem.* **2003**, *68*, 5681. (c) Medintz, I. L.; Trammell, S. A.; Mattoussi, H.; Mauro, J. M. *J. Am. Chem. Soc.* **2004**, *126*, 30.

(6) Lim, S.-J.; Seo, J.; Park, S. Y. *J. Am. Chem. Soc.* **2006**, *128*, 14542.

(7) (a) Kobayashi, N.; Lever, A. B. P. *J. Am. Chem. Soc.* **1987**, *109*, 7433. (b) Ushakov, E. N.; Gromov, S. P.; Fedorova, O. A.; Pershina, Y. V.; Alfimov, M. V.; Barigelletti, F.; Flamigni, L.; Balzani, V. *J. Phys. Chem. A* **1999**, *103*, 11188.

(8) (a) Jelley, E. E. *Nature* **1936**, *138*, 1009. (b) Scheibe, G. *Angew. Chem.* **1936**, *49*, 563. (c) Helz, A. H. *Adv. Colloid Interface Sci.* **1977**, *8*, 237.

(9) Kasha, M. *Radiat. Res.* **1963**, *20*, 55.

10.1021/ic7010056 CCC: $37.00
Published on Web 10/19/2007

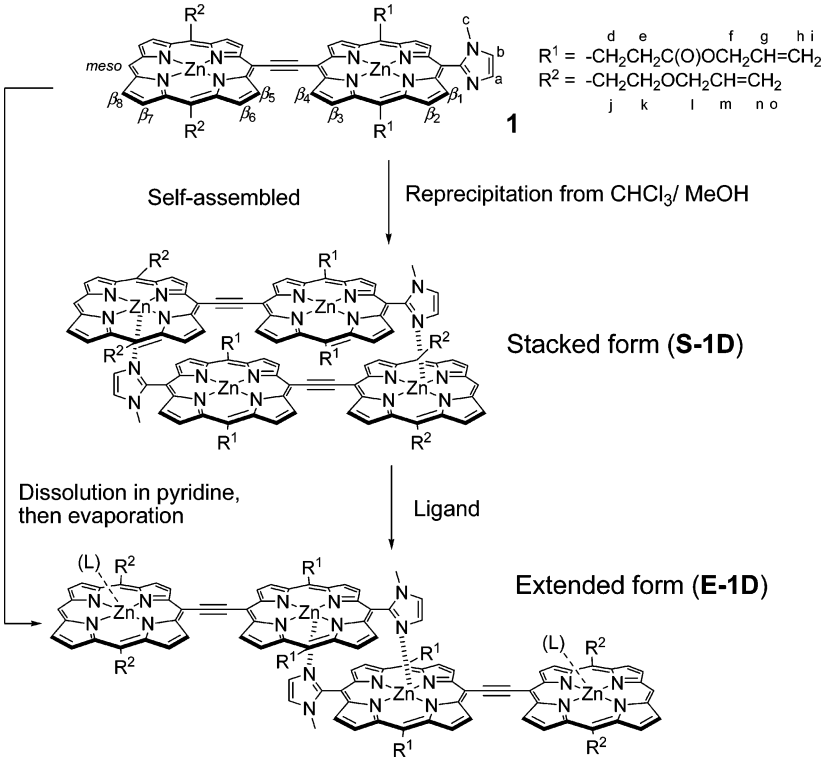

Figure 1. Structure of **1** and preparation of **S-1D** and **E-1D**.

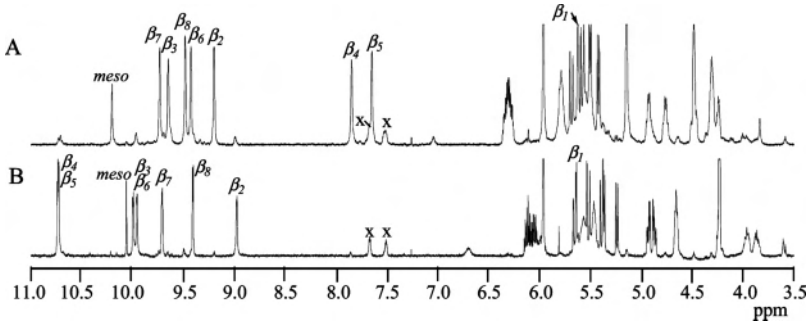

Figure 2. ^{1}H NMR spectra in $(CDCl_2)_2$ of (A) **S-1D** and (B) **E-1D**. Note: x indicates impurity.

aggregates, limiting their miniaturization to the molecular level. In this paper, we report controllable change of discrete molecular dimers that can be detected by fluorescence without the loss of structural integrity. *Stacked* and *extended* coordination dimers of bis(porphyrinatozinc) **1** are produced selectively by the control of ligand concentration and temperature. The extended dimer is more fluorescent than the stacked dimer and shows distinct chromism as well. Both the dimers are structurally defined by NMR analysis and clearly discriminated from obscure or indiscrete aggregates.

Results

^{1}H NMR Analysis. The synthesis of **1** has been reported previously.[13] The self-dimerization of **1** produces two structural isomers, stacked **S-1D** and extended **E-1D** (Figure 1). The **S-1D** dominant sample was prepared by reprecipitation of the mixture of **1** from chloroform and methanol, and **E-1D** was prepared selectively by evaporation of the **1D** mixture from pyridine. Gel permeation chromatographic (GPC) analysis of both **S-1D** and **E-1D** samples showed no polymeric species. The coordination dimer is formed dominantly under the preparation method. ^{1}H NMR spectra of **S-1D** and **E-1D** are shown in Figure 2 with assignments. The assignments of *meso*- and β-protons were carried out from HH−COSY (COSY = correlation spectroscopy) correlation and nuclear Overhauser effect (NOE) spectra (Figures S1−S3, Supporting Information). Adjacent β-proton pairs were recognized from the HH−COSY spectra of both

(10) (a) Maiya, G. B.; Krishnan, V. *Inorg. Chem.* **1985**, *24*, 3253. (b) Maiti, N. C.; Mazumdar, S.; Periasamy, N. *J. Phys. Chem. B* **1998**, *102*, 1528. (c) Screen, T. E. O.; Thorne, J. R. G.; Denning, R. G.; Bucknell, D. G.; Anderson, H. L. *J. Am. Chem. Soc.* **2002**, *124*, 9712. (d) Kameyama, K.; Morisue, M.; Satake, A.; Kobuke, Y. *Angew. Chem., Int. Ed.* **2005**, *44*, 4763.

(11) (a) Nakashima, N.; Kunitake, T. *J. Am. Chem. Soc.* **1982**, *104*, 4261, (b) Shimomura, M.; Kunitake, T. *J. Am. Chem. Soc.* **1987**, *109*, 5175.

(12) Kishimura, A.; Yamashita, T.; Yamaguchi, K.; Aida, T. *Nat. Mater.* **2005**, *4*, 546.

(13) Tanihara, J.; Ogawa, K.; Kobuke, Y. *J. Photochem. Photobiol., A* **2006**, *178*, 140.

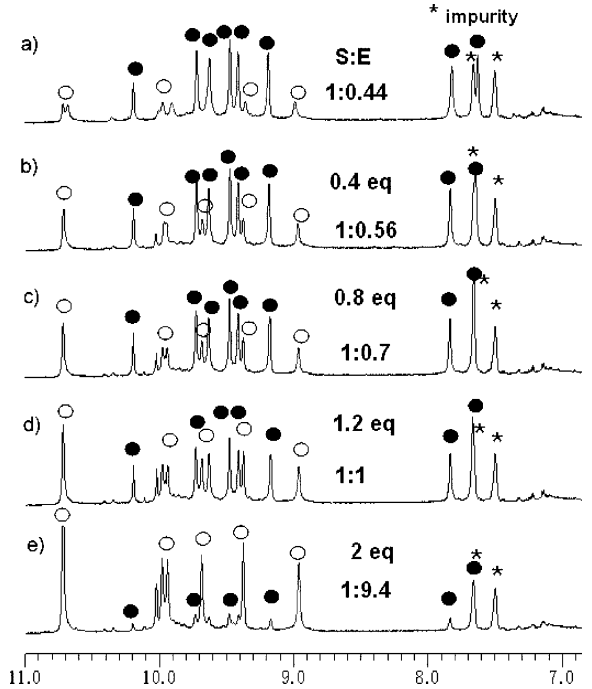

Figure 3. NMR titration of **S-1D** predominant sample (**S-1D**/**E-1D** = 1:0.44, 4.8 mM for monomeric unit **1**) with pyridine-d_5 (from top (a) to bottom (e): 0, 0.4, 0.8, 1.2, and 2 equiv with respect to **1**). **E-1D** dominant mixture (**S-1D′**/**E-1D′** = 1:9.4) was finally obtained as shown in the bottom (e). Key: open circle, **E-1D′**; filled circle, **S-1D′**).

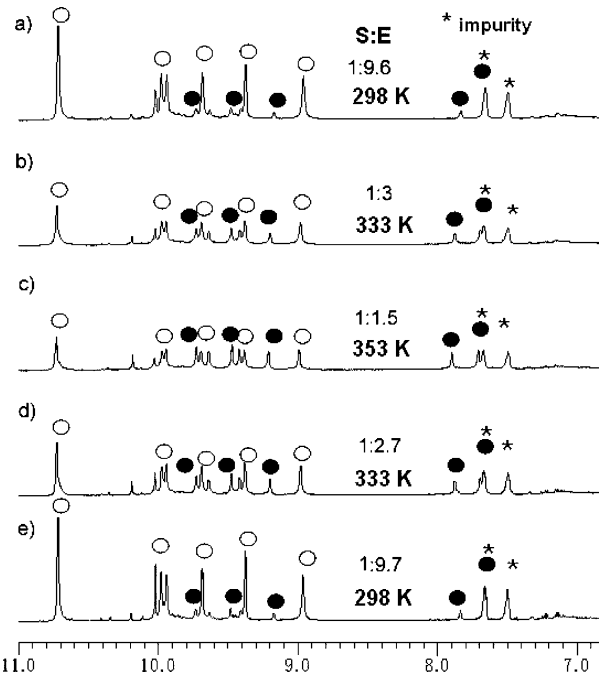

Figure 4. Equilibrium between **S-1D′** and **E-1D′** in temperature-variable ^{1}H NMR. (a) The same sample as that in Figure 3e at 298 K (**S-1D′**/**E-1D′** = 1:9.6), (b) 333 K (1:3), (c) 353 K (1:1.5), (d) 333 K (1:2.7), and (e) 298 K (1:9.7). The order of operation is from a to e.

samples. In both cases, β_1 protons are characteristically upper-field shifted (ca. 4 ppm) due to strong shielding effect from the coordinating complementary counterpart porphyrin.[14] The coupling partners β_2 were necessarily assigned. Then, β_8 protons of both samples were determined by NOE

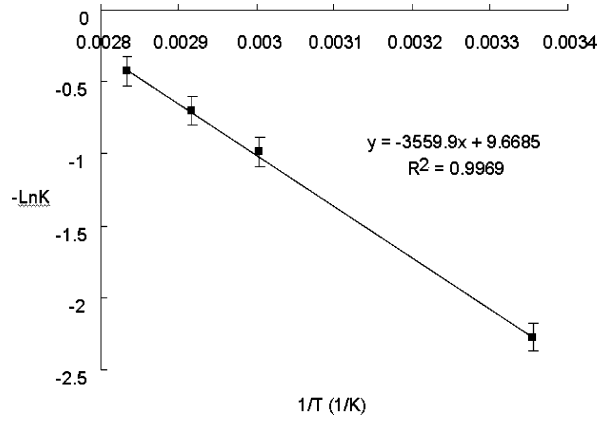

Figure 5. van't Hoff plots obtained from temperature-variable NMR.

correlation from each *meso*-proton. A big difference between parts A and B of Figure 2 is observed at the β_4 and β_5 protons area. In cases of ethynyl-linked bisporphyrins, these protons generally appear at fields lower than 10 ppm due to strong deshielding of the nearby porphyrin.[15] Therefore, chemical shifts of β_4 and β_5 protons in Figure 2B are close to typical values. The sample of 2B was assigned as **E-1D**.

However, those observed in Figure 2A are considerably shifted to upper-fields. When the peak at 7.86 ppm (indicated as β_4) was presaturated, NOE correlations were observed for the peaks at 7.65 (β_5, −61.7%), 9.22 (β_2), 9.44 (β_6), and 9.65 (β_3) ppm. When the peak at 7.65 ppm (indicated as β_5) was presaturated, NOE correlations were observed for the peaks at 7.86 (β_4, −57.3%), 9.22 (β_2), 9.44 (β_6), and 9.65 (β_3) ppm. Since no NOE correlation was observed between β_4 (and β_5) and β_2 in **E-1D**, the correlations observed in 2A are concerned with the facing porphyrin. From all of the NMR data, 2A was assigned as **S-1D**.

Ligand-Induced Transformation and Equilibrium. Transformation of **S-1D** occurs by the addition of coordinating ligands, yielding **E-1D′**, which contains 0, 1, and 2 equiv of ligands as **1D**, **1D-L**, and **1D-L$_2$**, respectively. An **S-1D** dominant sample (**S-1D**/**E-1D** = 1:0.44, 4.8 mM as **1** in $(CDCl_2)_2$) was titrated with pyridine-d_5. The addition of total 2 equiv of pyridine converted the sample to an **E-1D′** dominant species (**S-1D′**/**E-1D′** = 1:9.4) at 25 °C (Figure 3).[16] When the temperature of the sample was raised to 80 °C, the **S-1D′** composition increased. After cooling and standing at 25 °C for 15 h, the initial ratio was regenerated to confirm the equilibrium under the conditions (Figure 4), Thermodynamic parameters, ΔH −30 kJ/mol and ΔS −80 J/mol/K were obtained from the van't Hoff plot (Figure 5). It is noted that the values of thermodynamic parameters vary when the concentration of coordinating ligand is changed. In the NMR tube experiments, the error became relatively large among different experiments. Therefore, we do not discuss the values in detail. The important point is that both ΔH and ΔS were negative. Transformation of **S-1D′** into **E-1D′** is enthalpically favored, but entropically disfavored, suggesting that the added pyridine coordinates to the extended form more.

(14) Kobuke, Y.; Miyaji, H. *J. Am. Chem. Soc.* **1994**, *116*, 4111.

(15) Lin, V. S. Y.; Dimagno, S. G.; Therien, M. J. *Science* **1994**, *264*, 1105.

(16) **E-1D** and **E-1D-L$_2$** could not be distinguished by ^{1}H NMR.

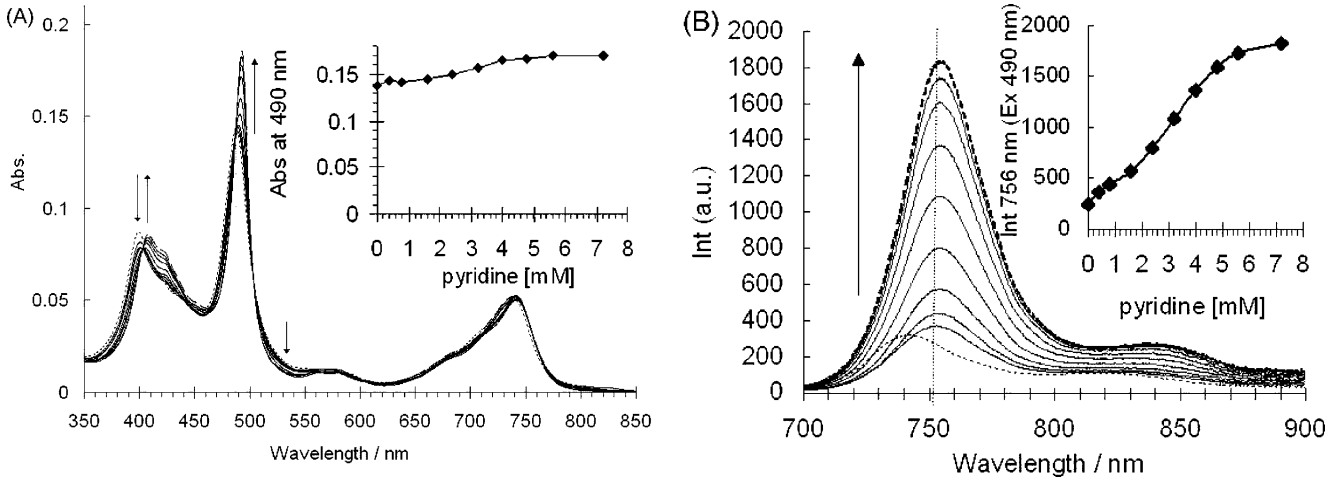

Figure 6. (A) UV−vis and (B) fluorescence titration (ex. 490 nm) of **S-1D** (1.6×10^{-6} M as monomer **1** in $(CHCl_2)_2$)) with pyridine. Dotted and broken lines indicate **S-1D** and **E-1D-py$_2$**, respectively. Insets: (A) absorbance at 490 nm and (B) fluorescence intensity at 756 nm as a function of added pyridine. The experimental points were joined as a line.

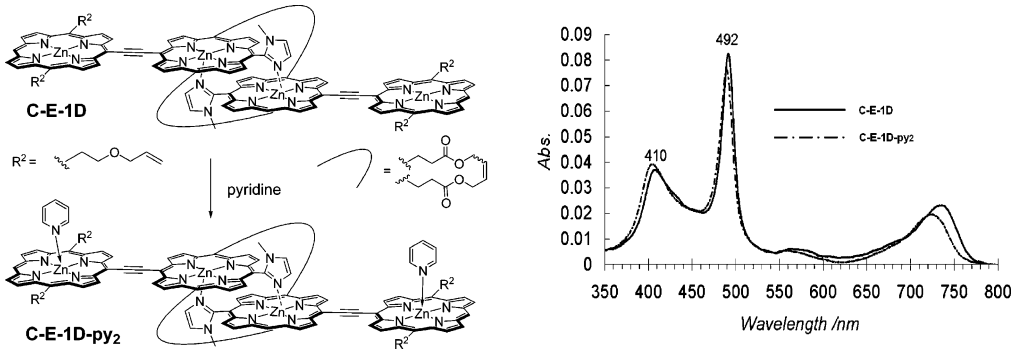

Figure 7. (left) Structures of covalently linked extended dimer **C-E-1D** and its pyridine adduct **C-E-1D-py$_2$**. (right) UV−vis spectra of **C-E-1D** (plain line) and **C-E-1D-py$_2$** (broken line) in $CHCl_3$.

Unfortunately, the coordinating pyridines were not detected by ^{1}H NMR even at −20 °C due to broadening and significant overlapping with other signals. NMR experiments indicate that pyridine coordination induces transformation from **S-1D** to **E-1D′**. Not only pyridine but also methanol and DMSO transform **S-1D** to **E-1D′**. A temperature-variable NMR study in the absence of coordinating ligand was also carried out to observe "real" isomerization between **S-1D** and **E-1D**. At high temperatures (up to 373 K), the ratio of **S-1D** to **E-1D** increased. However, the exchange rate at moderate temperature was too slow to obtain reliable dynamic and kinetic data.

Ligand-induced transformation was then monitored by UV−vis and fluorescence spectroscopies. An **S-1D** dominant sample (**S-1D**/**E-1D** = 10:1) was used as the starting compound. Spectral shapes at different concentrations (1.6×10^{-6} to 3.6×10^{-4} M) in 1,1,2,2-tetrachloroethane were identical, indicating that the dimer structure is maintained even at micromolar concentrations. This is compatible with the large association constant for the complementary coordination of imidazolyl to porphyrinatozinc.[14,17]

The UV−vis titration spectra (1.6×10^{-6} M of **1**) are shown in Figure 6A. To accelerate the attainment of equilibrium, the solution was heated first at 60 °C for 2 min

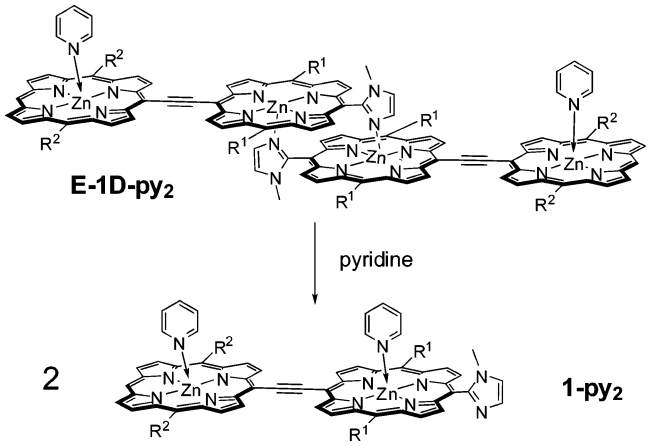

Figure 8. Dissociation of **E-1D-py$_2$** to monomeric **1-py$_2$**.

and the spectra were subsequently measured at room temperature (rt). At a concentration of 6 μM pyridine, the peak maximum of **S-1D** at 488 nm (dotted line) was red-shifted to 493 nm (broken line) and the spectral band became narrower. The final spectral shape and the peak positions are almost identical with those of covalently linked **C-E-1D-py$_2$**, which was prepared by the metathesis linking of **E-1D** followed by the addition of pyridine (Figure 7).[13,18]

(17) Satake, A.; Kobuke, Y. *Tetrahedron* **2005**, *61*, 13.

(18) Ohashi, A.; Satake, A.; Kobuke, Y. *Bull. Chem. Soc. Jpn.* **2004**, *77*, 365.

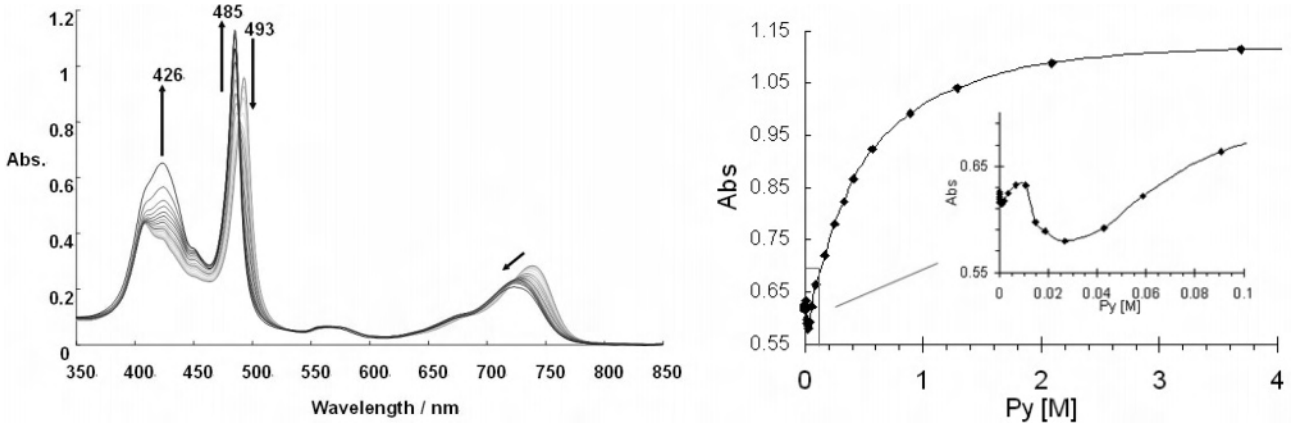

Figure 9. (left) UV−vis titration spectra of **E-1D-py$_2$** (8×10^{-6} M in $(CHCl_2)_2$) with large excess amounts of pyridine up to 4 M); (right) titration plot at 485 nm. The experimental points were joined as a line.

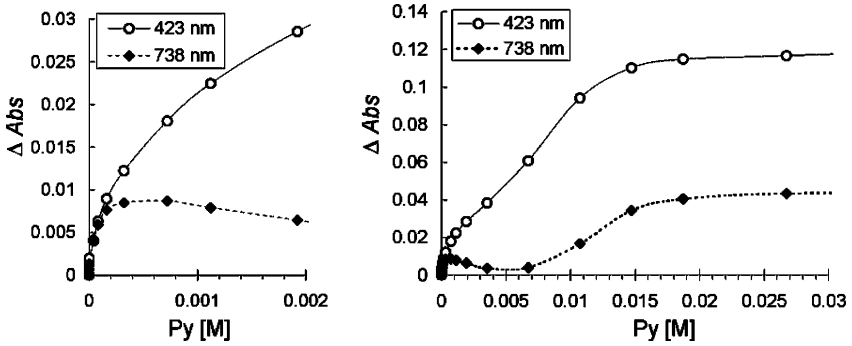

Figure 10. Absorption change of 423 and 738 nm as a function of added pyridine in the UV−vis titration of **S-1D** (4×10^{-6} M in $(CHCl_2)_2$) with pyridine *without heating* (see text). The experimental points were joined as a line.

Thus, the final spectrum in Figure 6A was assigned as the **E-1D-py$_2$** form. Further addition of pyridine (more than 40 mM) gradually produced monomeric **1-py$_2$** with the peak maximum at 485 nm, but more than 4 M of pyridine was required for complete dissociation (Figures 8 and 9). Judging from the titration plot at 485 nm in Figure 9, dimeric structures remained dominant up to 40 mM pyridine.

UV−vis spectral change from **S-1D** to **E-1D′** (Figure 6A) had no isosbestic point, and the titration plots did not vary monotonously. This behavior became more obvious when titration was carried out without heating. Figure 10 illustrates the titration plots of **S-1D** (4×10^{-6} M) to **E-1D′** at 738 and 423 nm. The spectra were collected after stirring for 5 min at 25 °C (no heating). Since the system does not reach equilibrium completely under the condition, kinetically stable intermediate(s) may appear. The absorbance change at 738 nm increased first until the addition of 0.2 mM pyridine and then decreased at the addition of 5 mM pyridine. It turned up again to give **E-1D-L$_2$** at the addition of 20 mM pyridine. When a heating process was inserted before each measurement, the decrease of the absorbance change around the addition of 5 mM pyridine became moderate. This nonmonotonous change suggests the existence of intermediates between **S-1D** and **E-1D-py$_2$**. This will be discussed later.

The fluorescence spectral change (ex. 490 nm) in the same titration of Figure 6A is shown in Figure 6B. After the transformation from **S-1D** to **E-1D-py$_2$**, a large enhancement of the fluorescence was observed, even though a much smaller absorbance change was detected at 490 nm (inset of part A). The fluorescence intensity at 756 nm increased approximately 7 times more than the corresponding absorbance increase of 1.23. The fluorescence quantum yields were determined to be 0.039 for **S-1D**, 0.105 for **E-1D-py$_2$**, and 0.083 for **1-py$_2$** in toluene.[19] In other words, the fluorescence intensity of **S-1D** is almost half the value for that of monomeric **1-py$_2$**, and that of **E-1D-py$_2$** is 2.5 times more fluorescent than that of **S-1D**. These fluorescent properties are compatible with the general tendency of *H*-

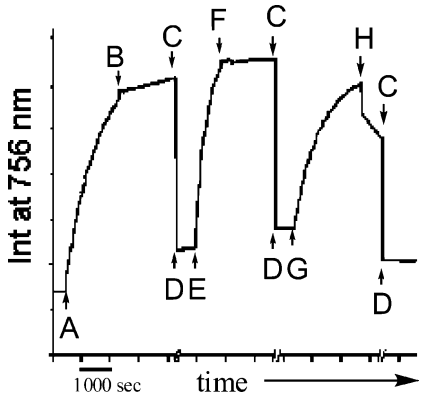

Figure 11. Time profile of fluorescence intensity (at 756 nm, ex. 492 nm, 25 °C): Starting point, **S-1D** (1.05×10^{-5} M as a monomer in $(CHCl_2)_2$ (2 mL)); A, add DMAP (5.25×10^{-4} M); B, add AcOH (5.25×10^{-4} M); C, pause measurement and heat at 70 °C for 30 min; D, restart measurement; E, add DMAP (3.15×10^{-3} M); F, add AcOH (2.8×10^{-3} M); G, add DMAP (2.1×10^{-2} M); H, add AcOH (500 μL). At the point of H, intensity decreased due to a dilution effect.

(19) ZnTPP (Φ_F 0.033 in benzene) was used as the reference.

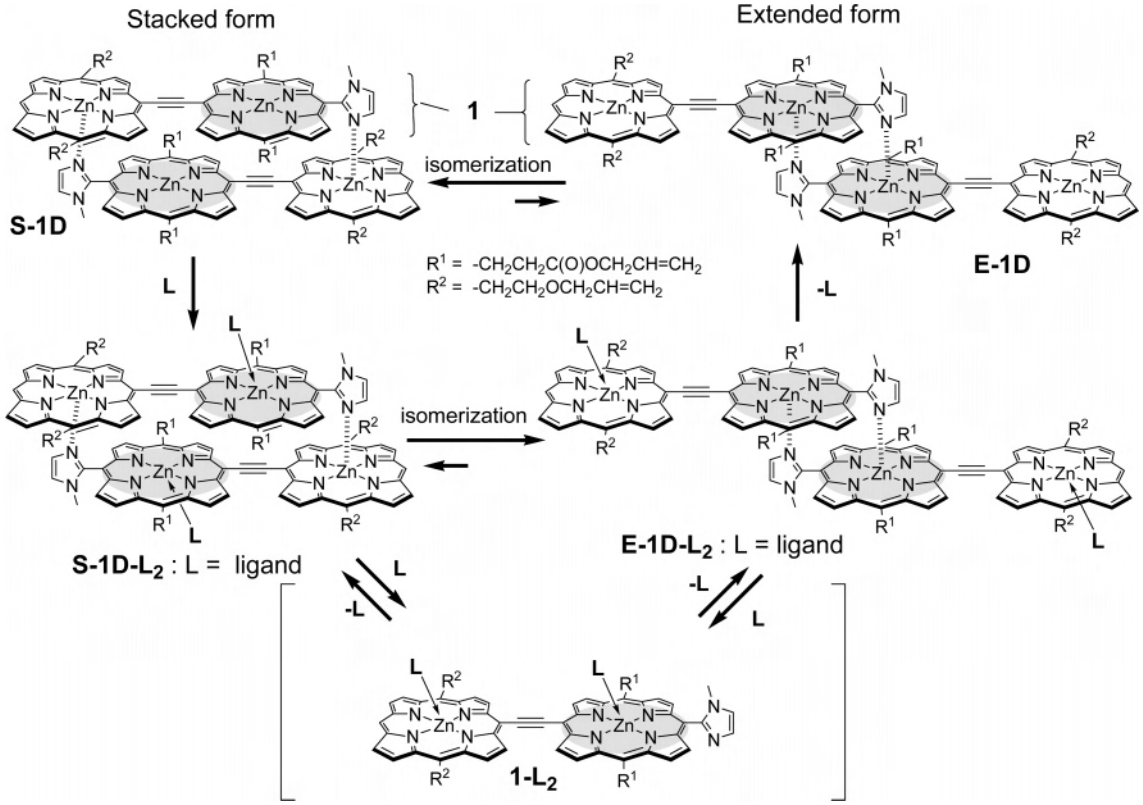

Figure 12. Proposed mechanism of interconversion among stacked and extended forms.

and *J*-aggregates of dyes, corresponding to S and E isomers, respectively.

Reversible Interconversion. To investigate the reversible interconversion of the stacked/extended isomers, 4-dimethylaminopyridine (DMAP) and acetic acid (AcOH) were added alternately. The system was monitored continuously by fluorescence intensity at 756 nm (ex. 492 nm). An **S-1D** dominant sample (**S-1D/E-1D** = 10:1, 1.05×10^{-5} M of **1** in $(CHCl_2)_2$) was used as the starting sample. The time profile is shown in Figure 11. When DMAP was added to the solution at point A to form a 5.25×10^{-4} M solution of DMAP, the fluorescence intensity gradually increased, suggesting progressive transformation from **S-1D** to **E-1D-py$_2$**. When AcOH was added to form a 5.25×10^{-4} M solution of AcOH at point B, the increase of fluorescence stopped. At point C, the sample was heated at 70 °C for 30 min in an oil bath. The fluorescence intensity measured at point D at rt had decreased considerably. At point E, DMAP was added again (3.15×10^{-3} M DMAP solution) to increase the fluorescence intensity until the next addition of AcOH at point F. This interconversion procedure was repeated twice. The operational interconversion clearly indicates the following: (1) The stacked (S) form is thermodynamically stable in the absence of ligand. (2) The extended (E) form becomes more stable in the presence of ligand. (3) The conversion rate is slow and the E to S conversion requires heating. The present system possesses a unique nonvolatile molecular memory, in which information is safely kept even after removal of the outer stimulus (ligand).

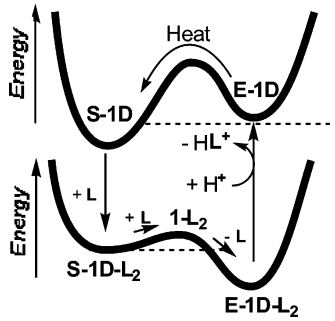

Figure 13. Approximate energy diagram among stacked and extended dimers.

Discussion

Mechanism of Interconversion. We propose a mechanism of interconversion among stacked and extended dimers (Figure 12). Three states, **S-1D**, **E-1D**, and **E-1D-L$_2$**, were observed directly in the experiment. **S-1D-L$_n$** (n = 1 or 2) must be formed kinetically, and they probably correspond to intermediates observed in Figure 10. Since conversion of the S to E forms requires the dissociation of two complementary coordination bonds, monomeric **1-L$_2$** may also form as a transient intermediate. At pyridine concentrations less than 40 mM, S to E conversion takes place. **1-L$_2$** is not observed significantly because complementary coordination is much more favored. However, the formation of **1-L$_2$** decreases the activation energy for the interconversion between **S-1D-L$_2$** and **E-1D-L$_2$**. The reverse conversion to the S isomer must be mediated first by the addition of AcOH to strip off the ligand to give **E-1D**. Although the **S-1D** isomer is thermodynamically more stable, **E-1D** exists stably

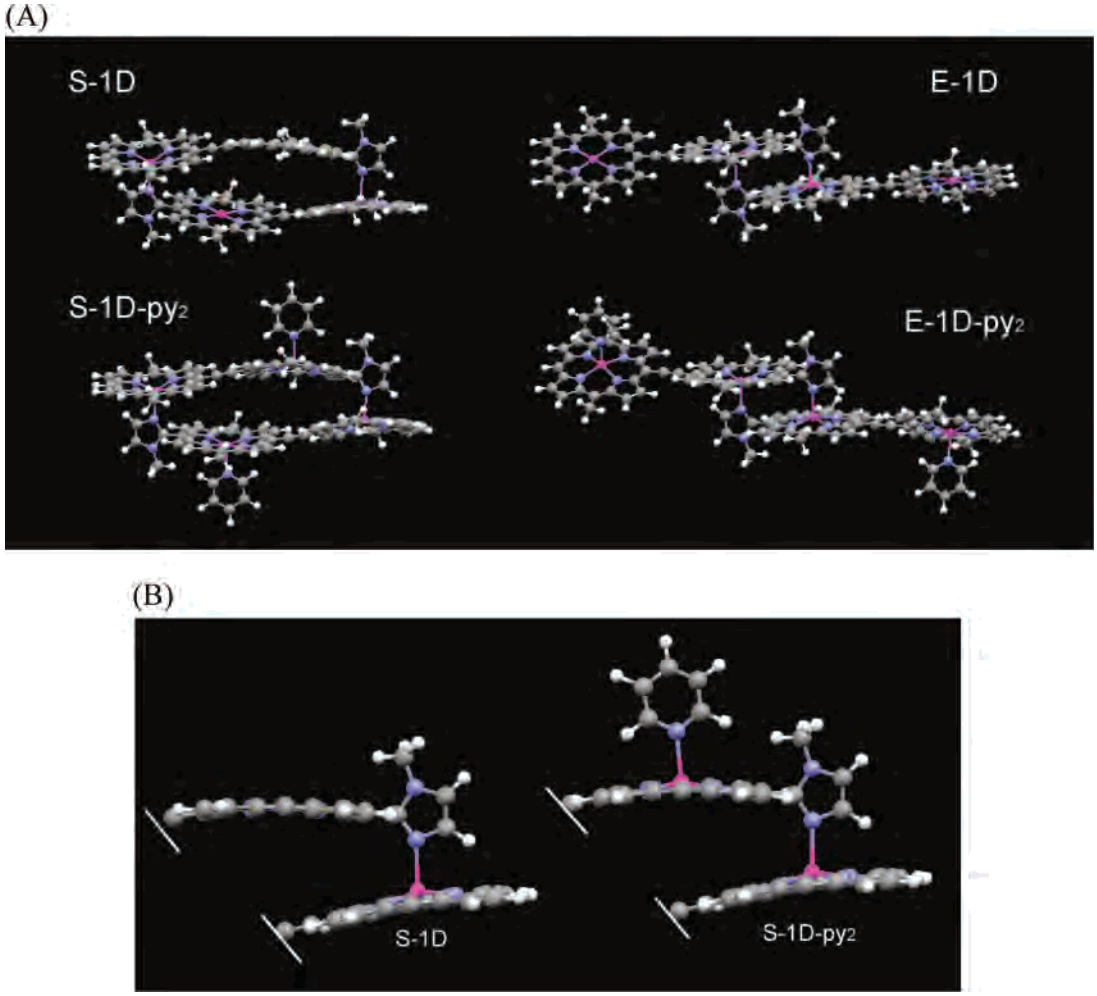

Figure 14. Molecular models of (A) **S-1D**, **S-1Dpy$_2$**, **E-1D**, and **E-1D-py$_2$** produced on *Materials Studio 4.0* (Accelrys, Inc.). Optimization of the geometry was carried out by a semiempirical MO method (AM1). Substituents at meso positions are replaced by methyl groups. (B) Magnified images of **S-1D** and **S-1Dpy$_2$**. The methyl groups are omitted for clarity.

at rt. Heat is required for the conversion to the S-form, suggesting that the activation energy from **E-1D** to **S-1D** is considerably high. A schematic image of the energy diagram of this four-component system is shown in Figure 13. Since the extended form is more fluorescent than the stacked one, the system is potentially useful for molecular memory applications.

Because of fluorescent nature of monomer **1-L$_2$**, interconversion between the stacked form and the monomer is another choice for molecular memory. However, large amounts of ligands (4−5 M for 1.6 μM of **1**) are required for the complete dissociation to the monomer from **E-1D-L$_2$**. The interconversion between the stacked and extended dimers is much conceivable.

Thermodynamic Stability of S and E Isomers. It is interesting to know the reason of apparently inverted stabilities between stacked and extended forms in the absence and presence of ligand. In the absence of ligand, the contribution of $\pi-\pi$ stacking may be dominant for stabilizing **S-1D** compared to **E-1D**. In the presence of enough ligands to be coordinated to most of the free zinc porphyrin sites, the equilibrium between **S-1D-L$_2$** and **E-1D-L$_2$** must be considered. On the basis of molecular modeling, the local geometry of the coordinating imidazolyl groups is changed from **S-1D** to **S-1D-L$_2$** so that the zinc ion adjacent to the imidazole is lifted toward the ligand by coordination (Figure 14). As a result, the $\pi-\pi$ stacking weakens and the coordination angle of imidazole must tilt further. The combined effects destabilize **S-1D-L$_2$** relative to **S-1D**. On the other hand, ligand coordination to **E-1D** may not affect the stability of **E-1D-L$_2$** because it occurs outside the complementary coordination. The relative destabilization of **S-1D-L$_2$** may contribute to the isomerization of **S-1D-L$_2$** to **E-1D-L$_2$**.

Conclusion

A unique interconvertible system was constructed on the basis of outer-stimuli-(ligands)-driven interconversion of coordination complexes, **S-1D** and **E-1D**. The stacked form (S) is thermodynamically more stable in the absence of ligand, whereas the extended form (E) is more stable in the presence of ligand. The E form is more fluorescent than the S form, and UV−vis spectral change was accompanied by the interconversion. By the combined use of these two properties, fluorescence intensity was increased by a factor of 7 by transformation from S to E forms. One could detect

the S or E form of even micromolar concentrations with high sensitivity by a fluorescence monitor. Since light irradiation does not induce, the information is repeatedly readable as fluorescence. Transformation from E to S required heating. Thus, the E form can be safely kept even after the removal of ligand. This feature is of potential utility for the development of nonvolatile molecular memory.

Experimental Section

General Methods. NMR spectra were obtained from JEOL ECP-600 (600 MHz) instruments. ^{1}H NMR chemical shifts are reported in parts per million (ppm) from the residual proton resonance ($(CHCl_2)_2$, 5.95 ppm) of the solvent as the internal standard. UV−vis spectra were obtained from a Shimadzu UV-3100PC instrument. Fluorescence spectra were obtained from a Hitachi F-4500 instrument. MALDI-TOF mass spectra were measured with a Applied Biosystems Voyager DE-STR apparatus. Dithranol purchased from SIGMA was used as a matrix in MALDI-TOF mass spectrometric measurements. Column chromatography was performed with silica gel (63-210 μm, KANTO chemical Co., Inc.). Thin layer chromatographies were performed on commercial Merck silica gel $60F_{254}$ plates. All other chemicals obtained from commercial sources were used without further purification, unless otherwise mentioned. The preparation of **1**, **S-1D**, **E-1D**, and **C-E-1D** was reported previously.[12]

Preparation of S-1D. Chloroform (3 mL) was added to a mixture (3 mg) of **S-1D** and **E-1D**. Most of the mixture was dissolved, but not completely. Methanol (5 mL) was added to the mixture, and the mixture was concentrated (to 5 mL approximately) until most of porphyrin was precipitated and the organic layer became almost colorless. The precipitate was collected on the membrane filter (Millipore poly(vinylidene fluoride), 0.1 μm). The brown solid was analyzed by ^{1}H NMR andGPC with a JAIGEL 3HA column (Japan Analytical Industry, polystyrene, exclusion limit 7×10^4 Da) by using $CHCl_3$ as an eluent. The GPC analysis showed no sign of polymer formation, but dimer as the sole product. The dominance of the **S-1D** sample (typically **S-1D**/**E-1D** = 10:1) is confirmed by NMR.

Preparation of E-1D. A sample (3 mg) of **S-1D** or a mixture of **S-1D** and **E-1D** was dissolved in pyridine (2 mL). The solution was evaporated by vacuum pump to give **E-1D** as dominant sample. A small amount of pyridine remaining coordinated might be enough to transform the dimer to the E form effectively.

Dissociated Monomer 1-py$_2$. A mixture (ca. 2 mg) of **S-1D** and **E-1D** was dissolved in pyridine-d_5 (0.4 mL) to give **1-py$_2$**. ^{1}H NMR (600 MHz, pyridine-d_5): δ 10.92 (br, 2H, Por-β-proton (β)), 10.89 (br, 2H, β), 10.24 (s, 1H, meso), 10.13 (br, 2H, β), 10.06 (br, 2H, β), 9.87 (d, 2H, J = 4.4 Hz, β), 9.70 (br, 4H, β), 9.54 (d, 2H, J = 4.4 Hz, β), 6.09−5.99 (m, 4H, CH═C), 5.72−5.64 (m, 4H, CH_2), 5.62−5.55 (m, 4H, CH_2), 5.43−5.35 (m, 4H, anti C═CH_2), 5.22 (d, 2H, J = 10.2 Hz, syn C═CH_2), 5.13 (d, 2H, J = 10.2 Hz, syn C═CH_2), 4.82 (br, 4H, CH_2), 4.75 (t, 4H, J = 7.2 Hz, CH_2), 4.43 (t, 4H, J = 7.2 Hz, CH_2), 4.21 (d, 2H, J = 4.4 Hz, CH_2), 3.66 (br, 3H, N−Me). Two imidazolyl peaks could not be detected due to overlapping with peaks of pyridine.

^{1}H NMR Titration. An **S-1D** dominant sample (3 mg) in $(CDCl_2)_2$ (0.5 mL) was transferred to an NMR sample tube. An NMR spectrum was recorded at 25 °C after each addition of pyridine-d_5 (99.5%, Aldrich) solution (0.25 M) in $(CDCl_2)_2$.

UV−Vis and Fluorescence Titration. UV−vis and fluorescence titrations shown in Figures 6A, 6B, and 9 were carried out in a Pyrex glass cuvette (band path 1 cm with a Teflon cap) filled with a **S-1D** dominant sample solution (1.6×10^{-6} M, 3 mL) in $(CHCl_2)_2$. Pyridine was added as a $(CHCl_2)_2$ solution initially and then directly to avoid the volume increase. The mixture was stirred for 2 min at 60 °C. UV−vis and fluorescence spectra of the solution were measured at 25 °C.

Molecular Modeling. Molecular mechanics calculation was performed on *Material Studio* (Accelrys, Inc.) using the universal force field.

Acknowledgment. This work was supported by Young Scientists (B) (A.S.) and Grant-in-Aids for Scientific Research (A) (Y.K.) from JSPS (Japan Society for the Promotion of Science).

Supporting Information Available: 2D HH−COSY and heteronuclear multiple-quantum coherence NMR spectra and NOE studies of **S-1D** and **E-1D**; ^{1}H NMR of **1-py$_2$**. This material is available free of charge via the Internet at http://pubs.acs.org.

IC7010056